Atypical Protonation States in the Active Site of HIV-1 Protease: A Computational Study

Paul Czodrowski, Christoph A. Sotriffer, and Gerhard Klebe*

Institut für Pharmazeutische Chemie, Philipps-Universität Marburg, Marbacher Weg 6, 35032 Marburg, Germany

Received November 20, 2006

The HIV protease (HIVP) is a prominent example for successful structure-based drug design. Besides its pharmaceutical impact, it is a well-studied system for which, as experimentally evidenced, protonation changes in the active site occur upon ligand binding. Therefore, it serves as an ideal candidate for a case study using our newly developed partial charge model, which was optimized toward the application of Poisson−Boltzmann based pK_a calculations. The charge model suggests reliably experimentally determined protonation states in the active site of HIVP. Furthermore, we perform pK_a calculations for two HIVP complexes with novel types of inhibitors developed and synthesized in our group. For these complexes, no experimental knowledge about the protonation states is given. For one of the compounds, containing a central pyrrolidine ring, the calculations predict that both catalytic aspartates should be deprotonated upon ligand binding.

1. INTRODUCTION

The Acquired ImmunoDeficiency Syndrome (AIDS) is a disease affecting the human immune system first characterized about 25 years ago. The causative agent of this disease is the retrovirus named Human Immunodeficiency Virus (HIV),[1] which appears in two forms, HIV-1 and HIV-2. The best-studied drug target of the virus is the HIV-1 protease (HIVP). Currently, there are eight approved drugs on the market that aim at the inhibition of HIVP (http://www.hiv.net). Besides its significant pharmaceutical relevance, HIVP is a prominent example for atypical protonation states in the active site.[2−5] In this context, atypical protonation means a nonstandard protonation, i.e., a protonated acid or a deprotonated base. We therefore selected this target to study the predictive power of Poisson−Boltzmann-based (PB-based) pK_a calculations using our newly developed PEOE_PB partial charge model.[6]

HIVP forms a symmetric homo-dimer, with each chain containing 99 residues. The central core of the dimer forms the active site (see Figure 1). The reaction catalyzed by HIVP is a peptide-bond cleavage, usually between a Tyr and a Pro or between a Phe and a Pro. The binding pocket is composed of the catalytic triad Asp-Thr-Gly. The two aspartates (one from each domain of the homo-dimer) are of main relevance and are therefore named the catalytic dyad. Besides the central cavity which is formed by the active site, three specificity pockets are accessible (S_1, S_2, and S_3; and due to symmetry, S_1', S_2', and S_3'). These specificity pockets preferably accommodate the hydrophobic parts of the ligand, which are named accordingly P_1, P_2, and P_3 (and P_1', P_2', and P_3', respectively).

Two design strategies have been followed in the development process of HIVP inhibitors: in the first generation, it was attempted to mimic the transition state by peptidomimetics mostly with one central hydroxylic group donating a hydrogen bond to the catalytic dyad. Inhibitors of the second generation contain a carbonyl group mostly embedded into a central ring moiety to displace the "flap water". The latter is a conserved water molecule hydrogen-bonding to the flap region via Ile50; the flap region of HIVP is the highly flexible part of the protein. This flap water is a special structural element unique for this viral protease. We will perform systematic studies on the inclusion or exclusion of this water molecule to study the relevance of explicitly considered water molecules for future pK_a calculations.

The five inhibitors that were considered in our study are shown in Figure 2. **KNI-272**, **VX-478**, and **S6** represent members of the first generation of HIVP inhibitors, while **DMP-323** and **S7** belong to the second generation. The ligand **DMP-323** induces a protonation change of the catalytic dyad: from the apo state with one of the two aspartates protonated[2,3] to a double-protonated state with both aspartates uncharged.[4] Thus, obviously HIVP displays already as apo enzyme an atypical protonation state for the catalytic dyad, which can be modulated upon ligand binding. The correct prediction of such effects displays the main focus of our computational study. We start with calculations for the uncomplexed and complexed HIVP where experimental data on the adopted protonation states are available. This will give insight into the power of our method to correctly predict protonation states and will serve as a benchmark study. Furthermore, we will face our results to a former computational pK_a study on HIVP complexes.[7] Finally, we will predict the protonation states for HIVP complexes where up to now no experimental data on the protonation states of the catalytic dyad have been recorded.

1.1. Setting of the Dielectric Constant and Handling of Coupled Systems. Prior to the discussion of possibly limiting factors, we will start with a brief introduction to PB-based pK_a calculations. Three different energy contributions to the ΔG of a protonation reaction are determinant for the final pK_a value and provoke the shift from the model pK_a value, pK_a^{mod} (corresponding to the pK_a value of the

* Corresponding author phone: 0049 6421 2821313; fax: 0049 6421 2828994; e-mail: klebe@staff.uni-marburg.de.

10.1021/ci600522c CCC: $37.00
Published on Web 05/16/2007

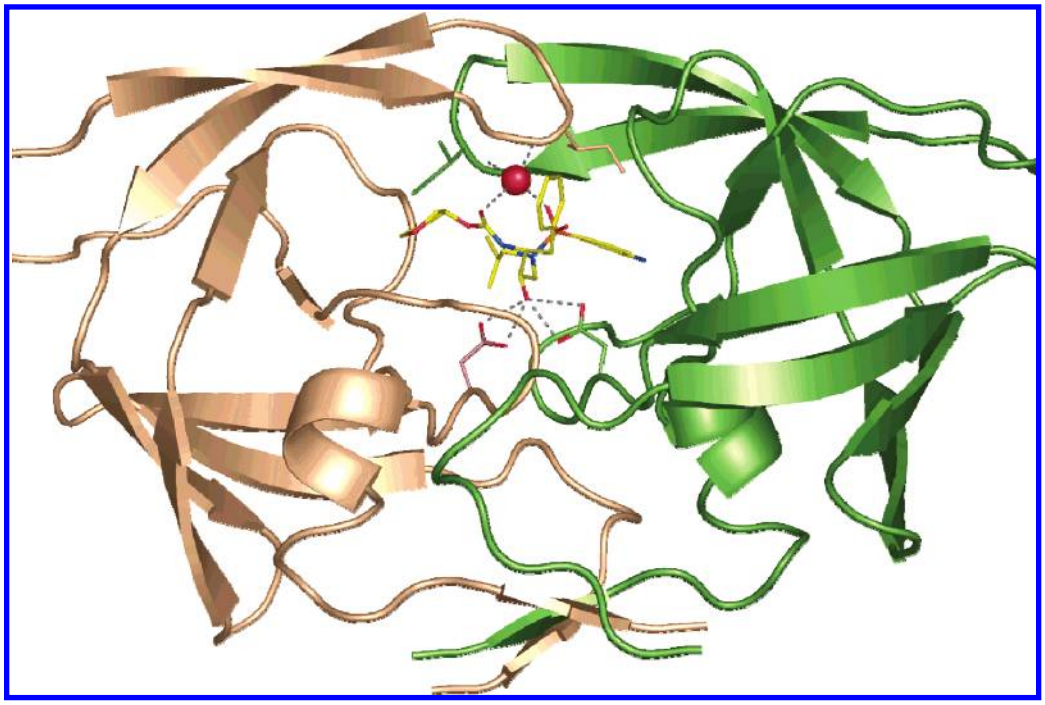

Figure 1. The complex formed by HIVP with the inhibitor **VX-478** (amprenavir, see Figure 2): the ligand, the catalytic dyad, and Ile50 of the flap region are shown in stick representation. The flap water, hydrogen-bonding to the backbone of Ile50, is given as a red sphere.

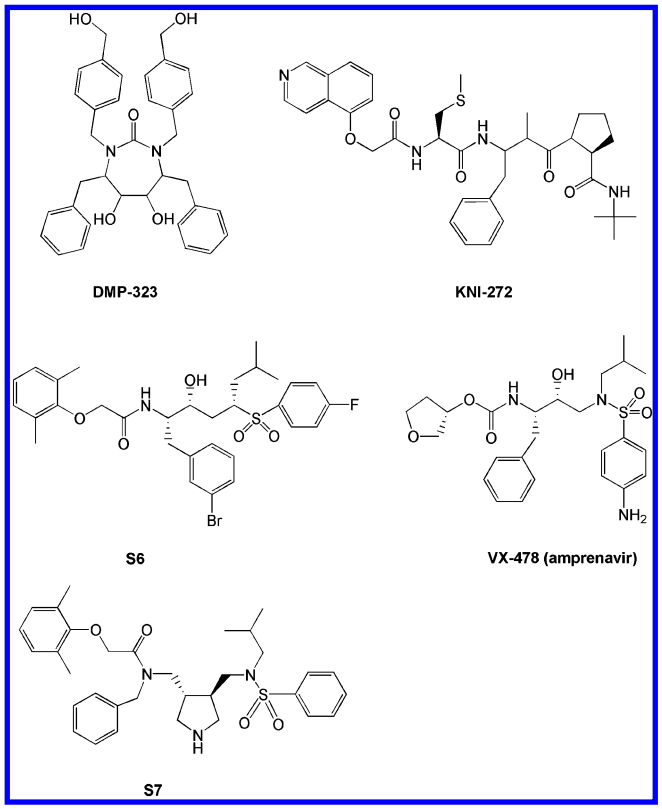

Figure 2. Inhibitors of HIVP used for the pK_a study: **DMP-323**, **KNI-272**, **S6**, **S7**, and **VX-478**.

isolated residue in aqueous solution), to the pK_a value in the actual protein environment: the solvation energy, the background interaction energy, and the site−site interaction energy. The solvation energy considers the penalty from the desolvation; the interaction with the permanently present dipoles and charges is represented by the background interaction; and the interaction of the titratable residues with each other is covered by the site−site interaction energy term. The first two quantities represent the *intrinsic* pK_a value (pK_a^{int}): although they are artificial (all titratable residues besides the one of interest are in the neutral state) and cannot be experimentally detected, they possibly indicate the predominance of one contribution. The consideration of the site−site interactions reveals the final pK_a value in the protein environment.

One central point of discussion with respect to pK_a calculations is the choice of the protein dielectric constant ($\epsilon_{Protein}$). The interested reader is referred to Warshel's excellent review on this topic.[8] In previous studies, it was shown that the best overall agreement (with the experimentally determined pK_a values) can be achieved setting $\epsilon_{Protein}$ to 20.[6,9] However, the analyses primarily involved solvent-exposed residues which show only minor pK_a shifts. For active-site residues experiencing large pK_a shifts, the assignment of $\epsilon_{Protein} = 4$ generates better results. This could be shown for lysozyme (Glu35: $pK_a^{exp} = 6.2$)[6,9] and xylanase (Glu172: $pK_a^{exp} = 6.7$).[6] Competitive studies illustrate a broad range of applied dielectric constants: Demchuk and Wade used in their PB-based pK_a calculations $\epsilon_{Protein}$ of 80 for solvent-exposed residues and 15 for desolvated sites.[10] Nielsen et al. used a single value of 8 for all residues.[11,12] King et al. found in microscopic MD simulation studies that the (macroscopic) dielectric constant could be as high as 10 in sites of catalytic importance.[13] This shows that there is no universal value for $\epsilon_{Protein}$. In order to validate our pK_a calculation methodology, and having experimental data for some of the studied complexes as a reference, we performed our pK_a calculations at three different values of $\epsilon_{Protein}$: 4, 10, and 20. These values cover a large range for the dielectric constant of the protein, and we hope in light of the experimental reference points to draw some conclusion concerning the preferred setting of $\epsilon_{Protein}$.

A second issue of pK_a calculations on HIVP structures concerns electrostatically strongly coupled systems. The two

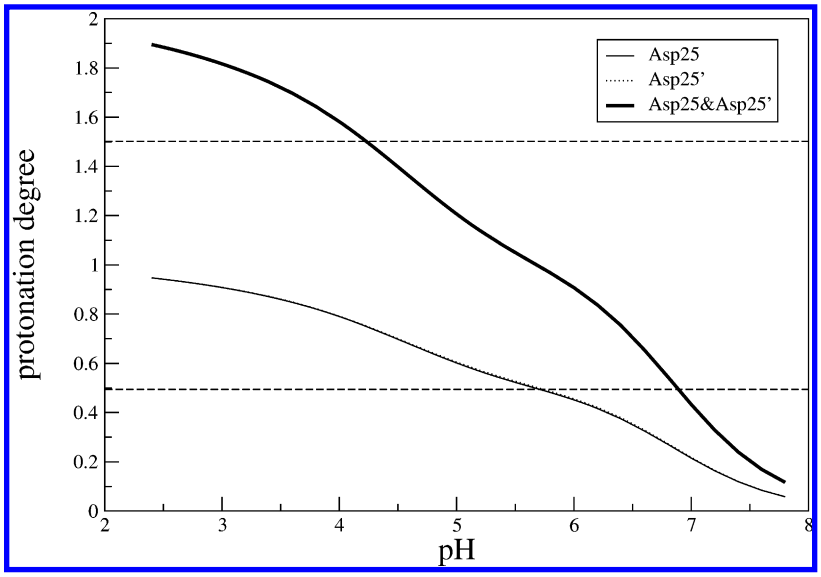

Figure 3. Titration curves of apo HIVP (crystal structure 1HHP, $\epsilon_{Protein} = 10$). The individual titration curves of the two aspartates, handled as independent are shown as thin (solid and dashed) lines; both curves are almost indistinguishable. The superimposed titration curve of the coupled diprotic acid system is given as thick line. The dashed straight lines at 1.5 and 0.5 correspond to situations of the coupled system where either 75% or 25% of both aspartates are protonated (corresponding pK_a values are here 4.22 and 6.89).

aspartates of the catalytic dyad undergo a strong mutual interaction on short distance resulting in such a system. This was previously reported in the pK_a study on HIVP of Trylska et al.[7] and can also be observed in our calculations. The two aspartates approach each other in space by approximately 3 Å. This proximity leads to the formation of a coupled system and results in a significant nonsigmoidal behavior (see Figure 3, thin lines). With respect to the computational setup, in the case of strongly coupled systems, it is necessary to perform a postprocessing step after the actual pK_a calculation. This was done in analogy to Trylska et al.,[7] who superimposed the single titration curves of Asp25 and Asp25′. This gives a titration curve similar to that of a diprotic acid, e.g., maleic acid. The pK_a values for the two aspartates correspond then to the situation where $\Sigma H^+ = 1.5$ and 0.5, corresponding to 75% or 25% protonation of the two coupled aspartates (see Figure 3, thick line and horizontal lines).

2. MATERIALS AND METHODS

MEAD was employed as PB solver.[14] The settings of the pK_a calculations and computational details of our PEOE_PB partial charges are given elsewhere.[6] PDB2PQR was used to generate hydrogens for the protein residues.[15] A direct comparison to our former model[6] for the simulation of the uncharged form of aspartate and glutamate in which implicit hydrogens were placed to model the neutral state showed an improvement when using explicit hydrogens instead. Therefore, we placed explicit hydrogens on the OD2 (Asp) and OE2 (Glu) atom. SYBYL was applied to add hydrogens to the ligands.[16] Manual adjustment of the considered local conformation was done for the central hydroxylic groups of the ligand being in close contact to the catalytic dyad (named "rot-scan"). Where available, experimental knowledge about the formed hydrogen bonds was used: this is the case for the symmetric cyclic urea compound **DMP-323**[4] and the asymmetric peptidomimetic **KNI-272**.[5] In case pK_a calculations were performed considering explicit water molecules, the orientation of the hydrogen atoms was manually adjusted.

To study the protonation effects upon ligand binding, two pK_a calculations are required: one without the bound ligand and a second with the bound ligand. The net protonation effect is the resulting difference between the degrees of protonation between the two forms. The protonation states are calculated at a pH of 5.0, as HIVP optimally catalyzes the peptide bond cleavage within a pH range of 4.0 and 6.0.[3] The notation H^+ is used for the protonation degree of one particular residue, i.e., $H^+ = 1.0$ corresponds to full protonation and $H^+ = 0.0$ to complete deprotonation. The notation ΣH^+ describes the sum of the protonation degrees of the two aspartates forming the catalytic dyad. The following crystal structures (given by their PDB codes) for complexed and uncomplexed HIVP structures were used: 1HHP (apo), 3HVP (apo), 1HPX (**KNI-272**), 1QBS (**DMP-323**), 1XL5 (**S6**), 1XL2 (**S7**), 1HPV (**VX-478**). The ligands are given in Figure 2.

The structural differences between the two apo structures are rather marginal: the C_α fit gives an root-mean-square deviation (rmsd) value of 0.40 Å, and both crystal structures show the same space group ($P4_12_12$). Their resolution is 2.7 Å (1HHP) and 2.8 Å (3HVP). A comparison of the apo structures and the complexes reveals C_α-rmsd values between 0.96 and 1.35 Å. The complexes are structurally more similar among each other: the rmsd lies between 0.47 and 0.77 Å. The resolution of the complexes is higher compared to the apo structures and ranges between 1.5 and 2.0 Å. The complexes appear in different space groups: $P2_12_12_1$ (1XL2), $P6_1$ (1QBS, 1HPV), $P2_12_12$ (1XL5).

We calculated pK_a values for the following titratable residues (predefined model pK_a values are given in parentheses): aspartate (4.0), glutamate (4.4), histidine (6.3), cysteine (8.7), tyrosine (9.6), lysine (10.4). The pK_a values of the C- and N-termini were not considered, since they are 18 Å apart from the catalytic dyad and assumed to remain in their standard protonation state upon complexation. With

Table 1. Comparison of HIVP Sequences[a]

position	1HHP/1HPX	3HVP	1QBS	1XL2/1XL5	1HPV
3	Ile	Ile	Val	Ile	Ile
14	Lys	Arg	Lys	Lys	Lys
37	Ser	Asn	Ser	Ser	Ser
41	Arg	Lys	Arg	Arg	Arg
63	Leu	Pro	Leu	Leu	Leu
64	Ile	Val	Ile	Ile	Ile
67	Cys	Aba	Cso	Cys	Cys
95	Cys	Aba	Ala	Cys	Cys

[a] Aba: α-amino-*N*-butyric acid; Cso: *S*-hydroxycysteine.

Table 2. Experimentally Determined pK_a Values for the Two Catalytic Aspartates in Apo HIVP[a]

ref	pK_{a1} (aspartate1)	pK_{a2} (aspartate2)
2	3.4−3.7	5.5−6.5
2	3.1−3.3	4.9−5.3
3	3.3	6.8

[a] The two ranges from ref 2 result from measurements on different substrates.

respect to the ligands, only **S7** contains a titratable group, which is a pyrrolidine ring.

In Table 1, the slight differences in the primary sequences of the evaluated HIV-1 proteases are listed. In the case of the 3HVP structure, all mutations to natural amino acids regard solvent-exposed residues and occur at least 16 Å from the catalytic dyad. Mutations to non-natural amino acids such as Aba and Cso (3HVP, 1QBS) are observed at least 10 Å apart from the catalytic center, and, thus, the influence on the catalytic dyad should be marginal. These residues (Aba, Cso) were mutated to cysteine for the pK_a calculations.

3. RESULTS

3.1. Calculations on Two Apo Structures. In Table 2, the experimentally determined pK_a values (determined via kinetic measurements) for apo HIVP are listed, which suggest monoprotonation for the catalytic dyad at a pH of 5.0. Whereas the experimental range for the first titration step of the coupled aspartates falls into a range between 3.1 and 3.7 the second step has been determined to occur between 4.9 and 6.8. The spread of nearly two log units makes a comparison to our computed results difficult. However, the protonation state at pH 5 appears well-characterized and suggests monoprotonation of the catalytic dyad. The results from NMR experiments[17] are not listed, since they only provide a range ($<$5.9) for both pK_a values.

The results of our pK_a calculations taking the two different apo protein structures (1HHP, 3HVP) as starting geometries are given in Table 3. They show that the computed results are in better agreement with the experimental values once the higher $\epsilon_{Protein}$ (20) is chosen. Decreasing the value of $\epsilon_{Protein}$ results in increasing pK_a differences between the two acids; in all cases, the difference is at least two log units. Nonetheless, the net protonation state of the two catalytic aspartates can be correctly predicted by five of the six pK_a calculations shown in Table 3. Thus, both starting geometries seem appropriate over a wide range of $\epsilon_{Protein}$ to correctly predict the monoprotonated state of the catalytic dyad at a pH of 5.0.

Table 3. pK_a Calculations on Two Apo HIVP (1HHP/3HVP)

							ref 7				
		aspartate1		aspartate2			aspartate1		aspartate2		
PDB	$\epsilon_{Protein}$	pK_{a1}	H^+ [a]	pK_{a2}	H^+ [a]	ΣH^+ [b]	pK_{a1}	H^+ [a]	pK_{a2}	H^+ [a]	ΣH^+ [b]
1HHP	4	6.06	0.92	9.90	1.00	1.92	3.4	0.02	6.9	0.99	1.01
	10	4.37	0.19	6.97	0.98	1.17					
	20	3.58	0.04	5.93	0.89	0.93	3.1	0.01	5.3	0.67	0.68
3HVP	4	4.83	0.40	9.69	1.00	1.40	2.1	0.00	6.7	0.98	0.98
	10	3.17	0.01	6.62	0.98	0.99					
	20	2.65	0.00	5.44	0.73	0.73	2.9	0.01	5.3	0.67	0.68

[a] Net degree of protonation of aspartate1 or aspartate2 at pH = 5. [b] Net degree of protonation of the dyad at pH = 5.

From a structural point of view, both apo structures are very similar: a C_α-fit reveals a rmsd of 0.4 Å. Similarly, the catalytic triad is structurally conserved: the rmsd values amount to 0.5 Å (Thr26), 0.59 Å (Asp25), and 0.06 Å (Gly27) after the C_α-fit for all C_α atoms. The distances between the oxygens of the catalytic dyad of the different apo structures vary by about 0.2 Å.

Similar PB-based pK_a-calculations were performed for several complexed and uncomplexed HIVP structures by Trylska et al.[7] For comparison, the results from this study are shown in the last two columns of Table 3. They used different values for $\epsilon_{Protein}$ in combination with two different charge models (full-charge: $\epsilon_{Protein} = 4$; single-site: $\epsilon_{Protein} = 20$). The single-site model handles ionization by adding ±1 point charge to one central atom[9] (using CHARMM22 charges and OPLS radii), whereas in the full-charge model the formal charges are distributed over several atoms[18] (using PARSE charges and radii). The latter treatment is more similar to our charge model. Using a dielectric constant of 20, the differences between our results and the study of Trylska et al. are smaller than one log unit. For the calculations with $\epsilon_{Protein} = 4$, larger deviations are observed.

3.2. Calculations for the Complexes. *3.2.1. Uncharged Symmetric Cyclic Urea.* **DMP-323** is a symmetric cyclic urea derivative which binds with a K_i-value of 340 pM.[19] Its benzyl moieties are accommodated in the S_1, S_1'-pockets, whereas the benzyl alcohol portions address the S_2, S_2'-pockets. The structural differences with respect to the apo HIVP structure (1HHP) are relatively large: the rmsd of the C_α-fit amounts to 1.35 Å. However, this difference is mostly provoked by the flap region, which is known to be rather adaptive.[20] The carbonyl group of the cyclic urea ring displaces the flap water, which was one of the initial goals in the development of this type of inhibitor.

The experimentally determined pK_a values of the two catalytic aspartates in the **DMP-323** complex are $>$7.2[4] suggesting that both residues are protonated at pH = 5. The pK_a values of all other aspartates and glutamates have also been determined by NMR experiments. Of these, only Asp29 deviates by more than one log unit from its model pK_a, exhibiting a pK_a value between 1.97 and 2.06. This lowered pK_a value is induced by the formation of salt bridges to Arg8 and Arg87′.

The results for the **DMP-323**/HIVP complex are given in Table 4. We focus mainly on the correct determination of the proton uptake upon ligand binding. To correctly predict this effect, $\Delta\Sigma H^+$ must be +1, since the catalytic dyad changes from monoprotonation to double-protonation upon

Table 4. pK_a Calculations on HIVP Complexed with **DMP-323** (1QBS)

	apo (ligand-deleted)					complexed with **DMP-323**					
	aspartate1		aspartate2			aspartate1		aspartate2			$\Delta\Sigma H^{+\,c}$
$\epsilon_{Protein}$	pK_{a1}	$H^{+\,a}$	pK_{a2}	$H^{+\,a}$	$\Sigma H^{+\,b}$	pK_{a1}	$H^{+\,a}$	pK_{a2}	$H^{+\,a}$	$\Sigma H^{+\,b}$	$\approx \Delta n$
4	5.79	0.86	10.19	1.00	1.86	9.96	1.00	20.34	1.00	2.00	+0.14
10	3.73	0.05	7.20	0.99	1.04	5.30	0.67	10.71	1.00	1.67	+0.63
20	2.97	0.01	5.95	0.89	0.90	3.62	0.04	7.06	0.99	1.03	+0.13

[a] Net degree of protonation of aspartate1 or aspartate2 at pH = 5. [b] Net degree of protonation of the dyad at pH = 5. [c] Net change of protonation upon ligand binding.

Table 5. Comparison with Results from Trylska et al. for the HIVP/**DMP-323** Complexes[a]

	HIVP complexed with **DMP-323**									
	PEOE_PB				ref 7				NMR[4]	
	pK_{a1}	$H^{+\,a}$	pK_{a2}	$H^{+\,a}$	pK_{a1}	$H^{+\,a}$	pK_{a2}	$H^{+\,a}$	pK_{a1}	pK_{a2}
$\epsilon = 4$	9.96	[1.00]	20.34	[1.00]	7.9	[1.00]	20.5	[1.00]	>7.2	>7.2
$\epsilon = 20$	3.62	[0.04]	7.06	[0.99]	3.6	[0.04]	6.5	[0.97]	>7.2	>7.2

[a] PEOE_PB stands for our charge model used throughout the pK_a calculations.

ligand binding. This quantity is comparable to Δn (molar net exchange of protons), which can be measured using ITC. In a previous study, we successfully predicted such Δn for a series of trypsin and thrombin complexes by means of similar pK_a calculations.[21] For the **DMP-323** complex, the uptake of additional protons is qualitatively correctly predicted, but quantitatively the full amount of one proton on molar ratio is not accurately estimated: we compute an uptake of +0.63 protons ($\epsilon_{Protein} = 10$). However, we consider this as a correct prediction of the trend. Furthermore, the pK_a shifts of the catalytic dyad for this $\epsilon_{Protein}$ amount to +1.6 and +3.5. Such changes can be considered as significant enough to assume protonation of both aspartates. Applying a dielectric constant of 4 or 20 the prediction is less satisfactory, though the correct direction of the pK_a shifts is suggested.

Also the downward pK_a shift of Asp29 is correctly predicted the results are given in (the Supporting Information). The difference between the experimentally determined pK_a value (between 1.97 and 2.06) and the calculated pK_a value is <0.5 log units, depending on the chosen dielectric constant.

A comparison of our results for the **DMP-323** complex with the study of Trylska et al. is given in Table 5. It can be seen that (using $\epsilon_{Protein} = 20$) the difference is less than one log unit. The aspartate with the lower pK_a value seems to be overestimated in our calculations at $\epsilon = 4$, while in the case of Trylska et al., the use of $\epsilon = 4$ gives better agreement with experiment, at least for the aspartate with the lower pK_a. Concerning the extreme pK_a values (>20), the authors argue that such values are unreasonable; nevertheless, also these calculations indicate that both residues definitely remain protonated.

3.2.2. Uncharged Asymmetric Inhibitor KNI-272. The asymmetric inhibitor **KNI-272** differs significantly from the cyclic urea compound studied in the previous section (see Figure 2). The inhibitor binds with a K_i of 5.5 pM.[22] Furthermore, only one hydroxylic group is placed between the two catalytic aspartates, qualifying **KNI-272** as member of the first generation of HIVP inhibitors. Two water molecules can be observed in the crystal structure: W301 and W607. W301 is the "flap water", and W607 is in close vicinity to one of the catalytic aspartates (with a distance of 3 Å). It forms a hydrogen bond to the ligand's hydroxylic group. We performed pK_a calculations both with and without W607 to probe its influence on the protonation states. The water molecule W301 was not included explicitly due to its large distance from the catalytic dyad.

Table 6. pK_a Calculations on HIVP Complexed with **KNI-272** (1HPX), with and without One Explicit Water Molecule (W607) in the Complexed Form

	apo (ligand-deleted)					complexed with **KNI-272** without W607					
	aspartate1		aspartate2			aspartate1		aspartate2			$\Delta\Sigma H^{+\,c}$
$\epsilon_{Protein}$	pK_{a1}	$H^{+\,a}$	pK_{a2}	$H^{+\,a}$	$\Sigma H^{+\,b}$	pK_{a1}	$H^{+\,a}$	pK_{a2}	$H^{+\,a}$	$\Sigma H^{+\,b}$	$\approx \Delta n$
4	5.98	0.89	11.10	1.00	1.89	5.51	0.76	28.71	1.00	1.76	-0.13
10	3.78	0.06	7.24	0.99	1.05	3.84	0.06	13.43	1.00	1.06	+0.01
20	2.93	0.01	5.88	0.88	0.89	3.1	0.01	7.99	1.00	1.01	+0.12

	apo (ligand-deleted)					complexed with **KNI-272** with W607					
	aspartate1		aspartate2			aspartate1		aspartate2			$\Delta\Sigma H^{+\,c}$
$\epsilon_{Protein}$	pK_{a1}	$H^{+\,a}$	pK_{a2}	$H^{+\,a}$	$\Sigma H^{+\,b}$	pK_{a1}	$H^{+\,a}$	pK_{a2}	$H^{+\,a}$	$\Sigma H^{+\,b}$	$\approx \Delta n$
4						5.20	0.61	29.63	1.00	1.61	-0.28
10						3.37	0.02	13.60	1.00	1.02	-0.03
20						2.71	0.01	7.98	1.00	1.01	+0.12

[a] Net degree of protonation of aspartate1 or aspartate2 at pH = 5. [b] Net degree of protonation of the dyad at pH = 5. [c] Net change of protonation upon ligand binding.

We explored the hydrogen-bond formation capability of the ligand's hydroxylic group to both aspartates by means of rotating the OH group in steps of 30 degrees ("rot-scan"). For each step, a pK_a calculation was performed. We observed dependencies on the calculated pK_a values: using $\epsilon_{Protein} = 20$, the pK_a value of one aspartate fluctuates within two log units, and that of the second by one log unit. In the crystal structure, the distance of the hydroxy oxygen amounts to 2.6 Å with respect to the carboxylate oxygen of the first aspartate, whereas the distance to the second displays a value of 3.1 Å. For the pK_a calculations presented in Table 6, an orientation of the ligand OH group has been considered which reveals the lowest pK_a for the proximate aspartate (Asp25 labeled in the crystal structure): in this orientation, a hydrogen bond can be formed to this aspartate. This evidence is in agreement with NMR experiment[5] where this aspartate forms two hydrogen bonds, one to W607 and a second to the ligand. The NMR experiment also revealed the pK_a values for the catalytic dyad; they were found to be <2.5 and >6.2 for the coupled system of the two aspartates.

This is in agreement with the predictions based on semiempirical quantum mechanical calculations that the system of aspartates is in a monoprotonated state once complexed with **KNI-272**.[23] In summary, all calculations suggest that the protease system remains in the same monoprotonated state upon complexation of the ligand **KNI-272**.

A comparison of the results in Table 6 shows that the presence or absence of the water molecule W607 can

Table 7. Comparison with Results from Ref 7 and Experimentally Determined pK_a Values

	HIVP complexed with **KNI-272**									
	PEOE_PB				ref 7				NMR[4]	
	pK_{a1}	$H^{+\,a}$	pK_{a2}	$H^{+\,a}$	pK_{a1}	$H^{+\,a}$	pK_{a2}	$H^{+\,a}$	pK_{a1}	pK_{a2}
$\epsilon = 4$	5.20	0.61	29.63	1.00	1.9	0.00	27.0	1.00	<2.5	>6.2
$\epsilon = 20$	2.71	0.01	7.98	1.00	4.5	0.26	7.0	0.99	<2.5	>6.2

[a] Net degree of protonation of aspartate1 or aspartate2 at pH = 5.

modulate the pK_a value of the proximal aspartate by up to 0.5 log units. However, this has only minor impact on the resulting protonation states and inventory. The influence of different orientations of the water molecule was not probed, but it is assumed that the influence is of minor importance, because an "ideal" hydrogen bond between the W607 and Asp25 has been modeled for our calculations.

In Table 7, we compare our results with those of Trylska et al.; the experimentally determined pK_a values are also listed. The results are similar for Asp25′, whereas large deviations are observed for Asp25. Suprisingly, opposing trends are suggested for both studies while decreasing $\epsilon_{Protein}$ from 20 to 4: in our case, the pK_a value of Asp25 is increased, whereas in the Trylska et al. study a decrease is suggested. Possibly in the latter study (which uses different charge models for the different dielectric constants) the PARSE charges show better performance for $\epsilon_{Protein} = 4$. Best agreement to experiment is achieved with our PEOE_PB charges using $\epsilon_{Protein} = 20$. Most importantly, all calculations suggest the overall trend correctly: the catalytic dyad remains in the monoprotonated state.

3.2.3. S6. The hydroxyethylene sulfone **S6** is another asymmetric inhibitor. The binding mode of its hydroxylic group resembles the binding mode of the central hydroxylic group of **KNI-272**. Inhibitor **S6** has been developed in our group and binds with a K_i of 45 nM.[24,25] Similar to the **KNI-272** complex, **S6** provokes different local environments next to the two aspartates of the catalytic dyad. Interestingly, a water molecule close to one of the aspartates is missing, although the **S6** and **KNI-272** structures are similar. No experimental data regarding the protonation states of the catalytic aspartates are available.

As the crystal structure determination cannot eludicate the orientation of hydrogens, the hydrogen-bonding partner of the ligand's hydroxy group is not fully characterized (both aspartates are close enough to form a hydrogen bond); the distance of the carboxylic oxygen amounts to 2.52 Å to the first aspartate and 2.61 Å to the second. Accordingly, we also performed a "rot-scan" of this ligand OH-group in steps of 30 degrees to detect the dependence of the pK_a values on the orientation of the OH group. For the results shown in Table 8, we selected an orientation in which the ligand's hydroxylic group forms a hydrogen bond to the proximal aspartate.

A comparison with the results from **KNI-272** shows that the pK_a value of the aspartate which is hydrogen-bonded to the ligand's hydroxylic group is much lower for the **S6**/HIVP complex. Most likely this is due to the shorter distance between the oxygen atoms of the hydrogen bond in the **S6** complex (2.52 Å) compared to the **KNI-272** complex (2.96 Å).

Table 8. pK_a Calculations on HIVP Complexed with **S6** (1XL5)

	apo (ligand-deleted)					complexed with **S6**					
	aspartate1		aspartate2			aspartate1		aspartate2			$\Delta\Sigma H^{+\,c}$
$\epsilon_{Protein}$	pK_{a1}	$H^{+\,a}$	pK_{a2}	$H^{+\,a}$	$\Sigma H^{+\,b}$	pK_{a1}	$H^{+\,a}$	pK_{a2}	$H^{+\,a}$	$\Sigma H^{+\,b}$	$\approx \Delta n$
4	4.05	0.10	11.95	1.00	1.10	-0.52	0.00	31.10	1.00	1.00	-0.10
10	2.13	0.00	7.24	0.99	0.99	0.53	0.00	15.20	1.00	1.00	+0.01
20	1.93	0.00	5.77	0.85	0.85	1.08	0.00	8.45	1.00	1.00	+0.15

[a] Net degree of protonation of aspartate1 or aspartate2 at pH = 5. [b] Net degree of protonation of the dyad at pH = 5. [c] Net change of protonation upon ligand binding.

Table 9. pK_a Calculations on HIVP Complexed with **VX-478** (1HPV)

	apo (ligand-deleted)					complexed with **VX-478**					
	aspartate1		aspartate2			aspartate1		aspartate2			$\Delta\Sigma H^{+\,c}$
$e_{Protein}$	pK_{a1}	$H^{+\,a}$	pK_{a2}	$H^{+\,a}$	$\Sigma H^{+\,b}$	pK_{a1}	$H^{+\,a}$	pK_{a2}	$H^{+\,a}$	$\Sigma H^{+\,b}$	$\approx \Delta n$
4	5.07	0.54	11.36	1.00	1.54	3.84	0.06	26.89	1.00	1.06	-0.48
10	3.45	0.03	7.29	0.99	1.02	2.71	0.01	12.52	1.00	1.01	-0.01
20	2.88	0.01	5.94	0.90	0.91	2.49	0.00	7.52	1.00	1.00	+0.09

[a] Net degree of protonation of aspartate1 or aspartate2 at pH = 5. [b] Net degree of protonation of the dyad at pH = 5. [c] Net change of protonation upon ligand binding.

The pK_a values resulting from our calculations must be seen in the light of the relative shifts. Hence, we can assume that a conserved monoprotonated state of the catalytic dyad seems most likely for the complexation with **S6**.

3.2.4. VX-478. In the design of **S6**, **VX-478** (now on the market and named amprenavir) was taken as a parent scaffold[24,25] bearing a similar central hydroxyl group. It binds with a K_i of 0.60 nM.[26] **VX-478** addresses the S_1 and S_2 (and S1′ and S_2′, respectively) pockets in a similar way as **S6**.

Analogous to the study of **KNI-272** and **S6**, we performed a "rot-scan" of the central ligand hydroxylic group to detect its optimal orientation. Regardless of the orientation, the catalytic dyad is in the monoprotonated state. We chose the orientation which revealed the lowest pK_a value for the deprotonated aspartate. The results are given in Table 9. Similar to the complexes with **KNI-272** and **S6**, we can assume that the catalytic dyad remains monoprotonated upon ligand binding.

3.2.5. S7. The ligand **S7** is another HIVP inhibitor that was developed in our group. It bears a pyrrolidine ring as new central core.[24,25] The (R,R)-enantiomer of **S7** binds with a K_i of 1.5 μM,[24,25] which makes it a weaker inhibitor than the other compounds studied in this contribution. One interesting structural feature is a water molecule, which is located in close vicinity of one of the two aspartates. The position of this water molecule is almost identical with the position of the water molecule W607 in the **KNI-272** complex.

The experimentally determined pK_a value for unsubstituted pyrrolidine amounts to 11.3;[27] we assigned a pK_a value of 11 for our calculations. We studied the charge setting for the neutral form of the pyrrolidine: either both hydrogens were "equally neutralized", or the charge of one of the bonded hydrogens was set to zero (the charge settings are shown in Figure 4, referenced as state I and state II). The state I model considers to some degree a possible dynamic

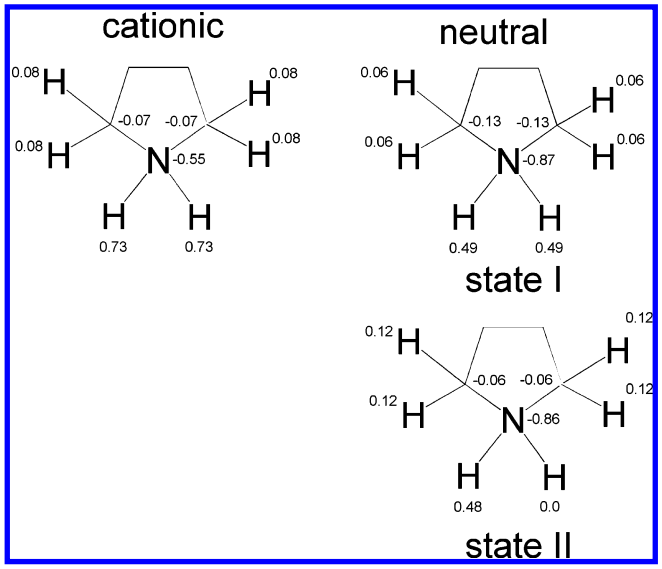

Figure 4. Charge settings for the neutral and charged states of the ligand **S7**.

fluctuation of the remaining hydrogen between the two orientations to the neighboring aspartates. However, both charge models produce similar pK_a predictions, which suggests that the van der Waals contribution on the pK_a values resulting from the *additional* hydrogen atom in state I is negligible. The results in Table 10 correspond to the state I model. The results suggest very low pK_a values for both aspartates. The large pK_a difference between the two aspartates can be explained by the asymmetric position adapted by the pyrrolidine ring. It approaches one of the aspartates 0.3 Å closer than the other. This aspartate reveals the lower pK_a value. In contrast, as expected for a strong salt bridge, the pK_a of the ligand nitrogen increases compared to the unbound state.

The influence of the explicit water molecule (named WAT98 in the PDB file) was also studied, and the results show a decreased pK_a value for the neighboring aspartate (labeled Asp25, see Table 10), which forms a hydrogen bond to this water molecule. However, this shift has no impact on the predicted protonation states.

Overall, the pK_a values of the two aspartates are shifted to a pK_a range where (at pH = 5) the catalytic dyad is supposedly fully deprotonated and, thus, present with two negatively charged carboxylate groups.

4. DISCUSSION

The two investigated apo crystal structures exhibit some deviations in the geometry, in consequence the computed pK_a values differ slightly. With increasing $\epsilon_{Protein}$ these differences decrease, an observation which correlates with a growing damping of the electrostatic interactions. For this reason larger $\epsilon_{Protein}$ values have been recommended as they better consider possible relaxations or local conformational multiplicity of the protein.[9] This might serve as an explanation why in general the values obtained with $\epsilon_{Protein} = 4$ deviate rather strongly from experiment. Furthermore, site−site interactions are responsible for the increased pK_a value of one of the catalytic aspartates in the apo structure. Possibly such site−site interactions are overestimated with $\epsilon_{Protein} = 4$, as too extreme pK_a values are predicted. Likely, again the electrostatic interactions on short distance are exaggerated.

The initial goal for this contribution was to benchmark our PEOE_PB charges, particularly to estimate changes of protonation states upon ligand binding. Experiments reveal the catalytic dyad to be monoprotonated for the uncomplexed enzyme. In case of the study of Trylska et al.,[7] this is only predicted using a $\epsilon_{Protein} = 4$. With our methodology, reasonable values are obtained with a setting of $\epsilon_{Protein} = 10$ or 20 for both apo structures. The use of different charge models provides a probable explanation for these differences.

As mentioned, the geometrical differences of the two apo structures result in somewhat deviating assignments of pK_a values. Nevertheless, the relative differences are similarly predicted. This observation points to a crucial aspect: What is the most reasonable approximation of the uncomplexed geometry, or, vice versa, by how much does the uncertainty in the reference geometry affect the accuracy of the computed pK_a calculations? It can be argued that a *ligand-deleted* structure of the protease is only a very approximate

Table 10. pK_a Calculations on HIVP Complexed with **S7** (1XL2)[d]

	apo (ligand-deleted)					complexed with **S7**						
						without one explicit water molecule						
	aspartate1		aspartate2			ligand	aspartate1		aspartate2			
$\epsilon_{Protein}$	pK_{a1}	H^+ [a]	pK_{a2}	H^+ [a]	ΣH^+ [b]	pK_a	pK_{a1}	H^+ [a]	pK_{a2}	H^+ [a]	ΣH^+ [b]	$\Delta\Sigma H^+$ [c] $\approx \Delta n$
4	5.40	0.72	10.48	1.00	1.72	27.38	-21.0	0.00	-4.55	0.00	0.00	-1.72
10	3.54	0.03	7.23	0.99	1.02	19.59	-9.60	0.00	-1.00	0.00	0.00	-1.02
20	2.92	0.01	5.97	0.90	0.91	16.66	-4.18	0.00	0.42	0.00	0.00	-0.91

	apo (ligand-deleted)					complexed with **S7**						
						with one explicit water molecule						
	aspartate1		aspartate2			lidand	aspartate1		aspartate2			
$\epsilon_{Protein}$	pK_{a1}	H^+ [a]	pK_{a2}	H^+ [a]	ΣH^+ [b]	pK_a	pK_{a1}	H^+ [a]	pK_{a2}	H^+ [a]	ΣH^+ [b]	$\Delta\Sigma H^+$ [c] $\approx \Delta n$
4						27.81	-21.00	0.00	-4.93	0.00	0.00	-1.72
10						19.59	-11.13	0.00	-1.17	0.00	0.00	-1.02
20						16.58	-4.85	0.00	0.32	0.00	0.00	-0.91

[a] Net degree of protonation of aspartate1 or aspartate2 at pH = 5. [b] Net degree of protonation of the dyad at pH = 5. [c] Net change of protonation upon ligand binding. [d] The model pK_a of the unbound **S7** is 11.0. The computations for the complexes were done with and without one explicit water molecule.

Table 11. Comparison of Mean pK_a Values for the Real Apo Structures and the *Ligand-Deleted* HIVP Structures

		mean pK_a^{apo}			mean p$K_a^{ligand-deleted}$		
		$\epsilon = 4$	$\epsilon = 10$	$\epsilon = 20$	$\epsilon = 4$	$\epsilon = 10$	$\epsilon = 20$
pK_{a1}	3.1−3.7	5.45	3.77	3.12	5.26	3.33	2.73
pK_{a2}	4.9−6.5	9.79	6.79	5.69	11.02	7.24	5.90

representation of the actual apo geometry; however, it is straightforward to produce. We want to compare the pK_a values obtained using different structures as input. In Table 11, the mean pK_a values averaged across the five different *ligand-deleted* structures are summarized. Facing them with the pK_a values obtained for the two experimental protein structures reveals a maximum deviation of 1.3 log units for $\epsilon_{Protein} = 4$. Considering the more reasonable settings of $\epsilon_{Protein} = 10$ or 20, the mean deviations reduce to 0.4 log units. As these deviations are smaller than the consequences of modifying the $\epsilon_{Protein}$ settings, the use of a *ligand-deleted* geometry appears a justifiable and very practical approximation for the intended calculations.

To predict the properties of the **DMP-323** complex, $\epsilon_{Protein} = 10$ seems to be optimal. The twofold protonation of the catalytic dyad is predicted correctly. Also for the **KNI-272** complex, $\epsilon_{Protein} = 10$ produces the best results. Here the protonation state of the catalytic dyad is estimated monoprotonated in agreement with experiment. A zero net uptake of protons is correctly predicted. The placement of an explicit water close to the catalytic dyad has only minor impact on the computed results.

The binding modes of **S6** and **VX-478** are rather similar, particularly with respect to the central hydroxylic group. Nonetheless, the resulting pK_a values of both aspartates reveal different pK_a values for the two complexes, particularly for $\epsilon_{Protein} = 4$. Independent of the actual values for $\epsilon_{Protein}$, however, the catalytic dyad is predicted to adopt monoprotonation, and zero uptake of protons is predicted upon complex formation.

The inhibitor **S7** induces a protonation pattern of the catalytic dyad which deviates from other complexes: both carboxy functions are predicted to be deprotonated. Although rather negative (most likely exaggerated) pK_a values are computed for both catalytic aspartates, the release of one proton upon complex formation is predicted, particularly for a setting of $\epsilon_{Protein} = 10$ or 20.

A central hydroxy group is present in the three ligands **KNI-272**, **S6**, and **VX-478**. Experimental evidence (by means of NMR measurements[5]) about the orientation of this hydroxy group is only available for the **KNI-272** complex. We explored different orientations of the hydroxy group by systematically scanning all rotamers. The hydrogen bond formation takes influence on the pK_a values of the catalytic dyad, as fluctuations of one to two pK_a units are observed. We selected the orientation that achieves the lowest pK_a value of all rotamers in agreement with experimental evidence.

5. CONCLUSIONS

Inhibitor binding to HIVP can induce a change of protonation of the two catalytic aspartates, as confirmed experimentally. We performed pK_a calculations on five different HIVP complexes and two apo structures. Depending on the type of ligand, different protonation states for the catalytic dyad are predicted. In cases where experimentally determined pK_a values are available our results have been compared to these reference values. Furthermore, a similar theoretical study[7] has been consulted for comparison. For the apo form of HIVP, the monoprotonated state of the catalytic dyad is evidenced by kinetic measurements.[2,3] Our calculations suggest very similar results either based on the geometry of two apo structures or of five complex structures from which the ligand has been removed. This fact underlines that the straightforward strategy of deleting the ligand from the complex structure is sufficiently accurate to produce relevant pK_a calculations (in case of HIVP).

The binding of **KNI-272** to HIVP involves no change of protonation of the catalytic dyad. The pK_a calculation correctly reproduces this experimental result. In contrast, upon binding of **DMP-323** one proton is picked up by the catalytic dyad. Also, this experimentally observed change is correctly reproduced by our calculations.

In the second part of the study, we have predicted protonation states of the catalytic dyad for three HIVP complexes where no experimental data on the protonation states are available. For the complexes with one central ligand hydroxyl group facing the dyad (**S6**, **VX-478**), the monoprotonated state is suggested. Most interestingly, for the **S7** complex with a formal positive charge on the central ligand's pyrrolidine moiety interacting with the dyad, both aspartates are predicted to occur in the deprotonated state. This protonation pattern has been proposed for HIVP complexed with the first generation inhibitor MVT-101.[28]

Knowledge about the most likely protonation state of ligands and protein residues is an important prerequisite to correctly set up computational drug design techniques such as docking and virtual screening. Possibly deviating settings can retrieve alternative hits since the assigned physicochemical properties (e.g., with respect to hydrogen-bond donor or acceptor functionalities) of the catalytic aspartates determine what type of ligand functional groups will be accepted as a potential binder of the protease. Furthermore, with respect to ITC experiments the present calculations can indicate whether superimposed changes of protonation might affect the measured heat signal. In case of overlaid protonation steps elaborate corrections have to be performed to obtain the net heat of binding which allows together with the recorded binding constant to factorize the binding affinity into enthalpic and entropic contributions.

ACKNOWLEDGMENT

Support of the present study by the bilateral research program CERC3 funded by CNRS and DFG (KL 1204/3) is gratefully acknowledged.

Supporting Information Available: All calculated pK_a values. This material is available free of charge via the Internet at http://pubs.acs.org.

REFERENCES AND NOTES

(1) Coffin, J.; Haase, A.; Levy, J. A.; Montagnier, L.; Oroszlan, S.; Teich, N.; Temin, H.; Toyoshima, L.; Varmus, H.; Vorgt, P.; Weiss, R. Human Immunodeficiency Virus. *Science* **1986**, *232*, 697−700.

(2) Hyland, L. J.; Tomaszek, T. A.; Meek, T. D. Human immunodeficiency virus-1 protease. 2. Use of pH rate studies and solvent kinetic isotope effects to elucidate details of chemical mechanism. *Biochemistry* **1991**, *30*, 8454−8463.

(3) Ido, E.; Han, H.; Kezdy, F. J.; Tang, J. Kinetic studies of Human Immunodeficiency Virus type 1 protease and its active-site hydrogen bond mutant A28S. *J. Biol. Chem.* **1991**, *266*, 24349−24366.
(4) Yamazaki, T.; Nicholson, K.; Torchia, D. A.; Wingfield, P.; Stahl, S. J.; Kaufman, J. D.; Eyerman, C. J.; Hodge, C. N.; Lam, P. Y. S.; Ru, Y.; Jadhav, P. K.; Chang, C.; Weber, P. C. NMR and X-ray evidence that the HIV-1 protease catalytic aspartyl groups are protonated in the complex formed by the protease and a non-peptide cyclic urea-based inhibitor. *J. Am. Chem. Soc.* **1994**, *116*, 10791−10792.
(5) Wang, Y. X.; Freedberg, D. I.; Yamazaki, T.; Wingfield, P. T.; Stahl, S. J.; Kaufman, D.; Kiso, Y.; Torchia, D. A. Solution NMR evidence that the HIV-1 protease catalytic aspartyl groups have different ionization states in the complex formed with the asymmetric drug KNI-272. *Biochemistry* **1996**, *35*, 9945−9950.
(6) Czodrowski, P.; Dramburg, I.; Sotriffer, C. A.; Klebe, G. Development, Validation, and Application of Adapted PEOE Charges to Estimate pKa Values of Functional Groups in Protein-Ligand Complexes. *Proteins* **2006**, *65*, 424−437.
(7) Trylska, J.; Antosiewicz, J.; Geller, M.; Hodge, C. N.; Klabe, R. M.; Head, M. S.; Gilson, M. K. Thermodynamic linkage between the binding of protons and inhibitors to HIV-1 protease. *Protein Sci.* **1999**, *8*, 180−195.
(8) Schutz, C. N.; Warshel, A. What are the Dielectric "Constants" of Proteins and How To Validate Electrostatic Models? *Proteins* **2001**, *44*, 400−417.
(9) Antosiewicz, J.; McCammon, J. A.; Gilson, M. K. Prediction of pH-dependent properties of proteins. *J. Mol. Biol.* **1994**, *238*, 415−436.
(10) Demchuk, E.; Wade, R. C. Improving the continuum dielectric approach to calculating pKas of ionizable groups in proteins. *J. Phys. Chem.* **1996**, *100*, 17373−17387.
(11) Nielsen, J. E.; McCammon, J. A. Calculating pKa values in enzyme active sites. *Protein Sci.* **2003**, *12*, 1894−1901.
(12) Joshi, M. D.; Sidhu, G.; Nielsen, J. E.; Brayer, G. D.; Withers, S. G.; McIntosh, L. P. Dissecting the electrostatic interactions and pH-dependent activity of a family 11 glycosidase. *Biochemistry* **2001**, *40*, 10115−10139.
(13) King, G.; Lee, F. S.; Warshel, A. Microscopic simulations of macroscopic dielectric constants of solvated proteins. *J. Chem. Phys.* **1991**, *95*, 4366−4377.
(14) Bashford, D. In *An object-oriented programming suite for electrostatic effects in biological molecules*; Scientific computing in object-oriented parallel environments, 1997; Ishikawa, Y., Oldehoeft, R. R., Reynders, J. V. W., Tholburn, M., Eds.; Springer: Berlin, ISCOPE97: 1997; pp 233−240.
(15) Dolinsky, T. J.; Nielsen, J. E.; McCammon, J. A.; Baker, N. A. PDB2PQR: an automated pipeline for the setup, execution, and analysis of Poisson-Boltzmann electrostatics calculations. *Nucleic Acids Res.* **2004**, *32*, 665−667.
(16) *SYBYL 7.0*; Tripos Inc.: St. Louis, MO, 2002.
(17) Smith, R.; Breton, I. M.; Chai, R. Y.; Kent, S. B. H. Ionization states of the catalytic residues in HIV-1 protease. *Nat. Struct. Biol.* **1997**, *3*, 946−950.
(18) Antosiewicz, J.; McCammon, J. A.; Gilson, M. K. The determinants of pKas in proteins. *Biochemistry* **1996**, *35*, 7819−7833.
(19) Lam, P. Y.; Ru, Y.; Jadhav, P. K.; Aldrich, P. E.; DeLucca, G. V.; Eyermann, C. J.; Chang, C. H.; Emmett, G.; Holler, E. R.; Daneker, W. F.; Li, L.; Confalone, P. N.; McHugh, R. J.; Han, Q.; Li, R.; Markwalder, J. A.; Seitz, S. P.; Sharpe, T. R.; Bacheler, L. T.; Rayner, M. M.; Klabe, R. M.; Shum, L.; Winslow, D. L.; Kornhauser, D. M.; Hodge, C. N. Cyclic HIV protease inhibitors: synthesis, conformational analysis, P2/P2′ structure-activity relationship, and molecular recognition of cyclic ureas. *J. Med. Chem.* **1996**, *39*, 3514−3525.
(20) Ishima, R.; Freedberg, D. I.; Wang, Y. X.; Louis, J. M.; Torchia, D. A.; Tung, R. D.; Navia, M. A. Flap opening and dimer-interface flexibility in the free and inhibitor-bound HIV protease, and their implications for function. *Structure* **1999**, *7*, 1047−1055.
(21) Czodrowski, P.; Sotriffer, C. A.; Klebe, G. Protonation changes upon ligand binding to trypsin and thrombin: Structural interpretation based on pKa calculations and ITC experiments. *J. Mol. Biol.* **2007**, *367*, 1347−1356.
(22) Mimoto, T.; Kiso, Y. Kynostatin (KNI)-227 and 272, highly potent anti-HIV agents: conformationally-constrained tripeptide inhibitors of HIV protease containing allophenylnorstatine. *Chem. Pharm. Bull.* **1992**, *40*, 2251−2253.
(23) Baldwin, E. T.; Bhat, N.; Gulnik, S.; Liu, B.; Topol, I. A.; Kiso, Y.; Mimoto, T.; Mitsuya, H.; Erickson, J. W. Structure of HIV-1 protease with KNI-272, a tight-binding transition-state analog containing allophenylnorstatine. *Structure* **1995**, *3*, 581−590.
(24) Specker, E.; Böttcher, J.; Brass, S.; Heine, A.; Lilie, H.; Schoop, A.; Müller, G.; Griebenow, N.; Klebe, G. Unexpected novel binding mode of pyrrolidine-based aspartyl protease inhibitors: design, synthesis and crystal structure of HIV protease. *ChemMedChem.* **2006**, *1*, 106−117.
(25) Specker, E.; Böttcher, J.; Heine, A.; Sotriffer, C. A.; Lilie, H.; Schoop, A.; Müller, G.; Griebenow, N.; Klebe, G. Hydroxyethylene sulfones as new scaffold to address aspartic proteases: design, synthesis and structural classification. *J. Med. Chem.* **2005**, *48*, 6607−6619.
(26) Kim, E. E.; Baker, C. T.; Dwyer, M. D.; Murcko, M. A.; Rao, B. G.; Tung, R. D.; Navia, M. A. Crystal structure of HIV-1 protease in complex with VX-478, a potent and orally bioavailable inhibitor of the enzyme. *J. Am. Chem. Soc.* **1995**, *117*, 1181−1182.
(27) Cabani, S.; Conti, G.; Lepori, L. Thermodynamic study on aqueous dilute solutions of organic compounds. *Trans. Faraday Soc.* **1971**, *67*, 1933−1942.
(28) Harte, W. E.; Beveridge, D. L. Prediction of the Protonation States of the Active Site Aspartyl Residues in HIV-1 Protease-Inhibitor Complexes via Molecular Dynamics Simulation. *J. Am. Chem. Soc.* **1993**, *115*, 3883−3886.

CI600522C